New Jersey Institute of Technology

Digital Commons @ NJIT

Spring 5-31-2008

Synthesis and analysis of carbon nanowalls and their raman spectroscopy

Amit Mahajan
New Jersey Institute of Technology

Follow this and additional works at: https://digitalcommons.njit.edu/theses

Part of the Electrical and Electronics Commons

ABSTRACT

SYNTHESIS AND ANALYSIS OF CARBON NANOWALLS
AND THEIR RAMAN SPECTROSCOPY

by
Amit Mahajan

Growth of Carbon Nanowalls has been carried out by Radio Frequency Chemical Vapor Deposition (RF-PECVD) on various substrates. Hydrogen was used as an active gas for the growth where as Ethanol bubbled with Argon was used as carbon source for formation of Carbon Nanowalls (CNW). The growth was then confirmed by Raman Spectroscopy and Scanning Electron Microscope (SEM) images. Also the need of using catalyst in CNW has been analyzed. The intensities of D and G bands obtained from Raman spectrum have been related to the length of Graphene walls, to study the CNW's length on different substrates.

The growth was carried on three substrates; Silicon wafer, Silicon wafer coated with Nickel Formate Dihydrate (NFD) as a catalyst.and Pure Nickel foil. It has been found that the catalyst does not play much important role in the growth of Carbon Nanowalls. Also it has been determined that Graphene sheets are the basic building blocks for nanowalls and the Graphene walls obtained in our experiment comprise only of one to two Graphene sheets. The morphologies of the growth of Carbon Nanowalls have been studied on the three substrates using SEM images. The growth of CNW in case of Silicon substrate and Silicon substrate having catalyst was found to be only in that direction and places, where the gases were passing these substrates. But in case of Nickel foil CNWs were found over the whole substrate that might be resulting because of Nickel itself acting as an active catalyst for the whole surface.

SYNTHESIS AND ANALYSIS OF CARBON NANOWALLS
AND THEIR RAMAN SPECTROSCOPY

by
Amit Mahajan

A Thesis
Submitted to the Faculty of
New Jersey Institute of Technology
in Partial Fulfillment of the Requirements for the Degree of
Master of Science in Electrical Engineering

Department of Electrical and Computer Engineering

May 2008

Blank Page

APPROVAL PAGE

SYNTHESIS AND ANALYSIS OF CARBON NANOWALLS
AND THEIR RAMAN SPECTROSCOPY
Amit Mahajan

Dr. Zafar Iqbal, Thesis Co-advisor   Date
Research Professor of Chemistry and Environmental Science, NJIT

Dr. Marek Sosnowski, Thesis Co-advisor   Date
Professor of Electrical and Computer Engineering, NJIT

Dr. Haim Grebel, Committee Member   Date
Professor of Electrical and Computer Engineering, NJIT

BIOGRAPHICAL SKETCH

Author: Amit Mahajan

Degree: Masters of Science

Date: May 2008

Undergraduate and Graduate Education:

- Masters of Science in Electrical Engineering,
  New Jersey Institute of Technology, Newark, NJ, 2008

- Bachelors of Technology in Electronics and Telecommunication Engineering,
  Chitkara Institute of Engineering and Tech, Chandigarh, Punjab India, 2006

Major: Electrical Engineering

To my beloved family

For their support and love.

ACKNOWLEDGMENT

I would like to express my deep and sincere gratitude to Dr. Zafar Iqbal, for his encouragement, support and guidance during the whole Thesis. I would also thank him for financially supporting me and being such a wonderful person to work with. Special appreciation and thanks to my advisor Dr. Marek Sosnowski for being a member of the research team and encouraging me during the whole project.

I would also thank Dr. Haim Grebel for being a member of Committee and appreciate him for providing us with all the useful resources. And note of thanks to Dr. Amit Goyal, Dr. Cris Wang, Mrs Anitha, Mrs Anna and Jinwen for their help during the entire project.

TABLE OF CONTENTS

.

CHAPTER 1

INTRODUCTION

1.1 OBJECTIVES

The objective of this study carried out at the Thin Film and Ion Beam Laboratory and the Carbon Nanotube and Fuel Cell Laboratory at the New Jersey Institute of Technology (NJIT) was to investigate a facile growth process, formation mechanism and structure of the new carbon form referred to as carbon nanowalls (CNWs), which is believed to be comprised of vertically aligned bundles of the two-dimensional allotropic form of carbon known as graphene. Field emission scanning electron microscopy (FE-SEM) and Raman spectroscopy were used to study the structure of the CNWs.

1.2 Carbon Allotropes

Carbon plays a unique role in chemistry and materials science. The ability of carbon atoms to form complicated networks is fundamental to organic chemistry and the basis for the existence of known forms of life. Even elemental carbon demonstrates unusually complicated behavior, forming a number of very different allotropic structures. As well as diamond and graphite, which have been known since ancient times, recently discovered fullerenes and nanotubes are currently the focus of attention in the emerging field of nanotechnology.

Carbon allotropes can be classified in terms of their spatial dimensionality. In this classification scheme fullerenes are zero-dimensional, carbon nanotubes are one dimensional, and diamond and graphite are three-dimensional, although graphite is well-known to have a layered structure with weak bonding between the layers [1]. A two-dimensional form of carbon allotropes which was conspicuously missing and previously named graphene, has been recently prepared by peeling single carbon layers from graphite [2], by chemically removing or etching silicon from the silicon carbide surface layer of a SiC single crystal [3] or by exfoliation of a graphite oxide followed by reduction [4]. Graphene layers thus prepared have been extensively investigated and found to have very exciting new electronic properties [5].

a) Three-dimensional Allotropes.

Diamond: It is one the best known allotropes of carbon, whose hardness and high transparency to light makes it useful for a wide range of industrial applications and as a gem. Each carbon atom in diamond is covalently bonded to four other carbons in a tetrahedron. The tetrahedra are then linked to form a 3-dimensional network (Figure 1.1) of puckered six-membered rings of atoms. This stable network of covalent bonds and the three dimensional arrangement of bonds makes diamond the hardest of all known materials.

Graphite: It is the most common allotrope of carbon. Unlike diamond, which is a good insulator in its undoped form, graphite is a semi-metal, and is widely used as an electrode in battery and electrochemical applications. Graphite has a layered structure (Figure. 1.1)

which is held together in three dimensions by weak inter-layer bonding. Figure 1 below

shows the arrangement of the atoms in each layer, and the way the layers are spaced.
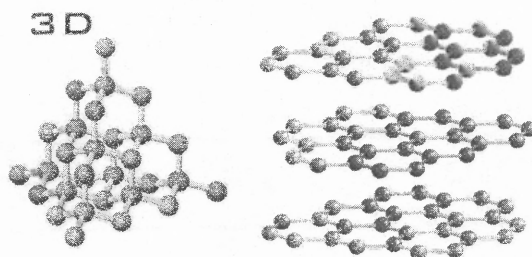
Figure 1.1 Three-dimensional structural packing of diamond (left) and graphite (right) [6].

b) Two-dimensional Allotropes.

Graphene: It is the name given to a flat monolayer of carbon atoms tightly packed into a

two-dimensional (2D) honeycomb lattice, and is the 2D basic building block for graphitic

materials of all other dimensionalities. It can be wrapped up into zero-dimensional

fullerenes after introducing five-membered rings into the soccer-ball shaped fullerenes,

rolled into one-dimensional nanotubes or stacked into the three-dimensional graphite

structure [14]. We suggest that it is also the building block in the formation of carbon

nanowalls based on the experimental results presented in this thesis. A perfect graphene

would consist exclusively of hexagonal cells as shown below in Figure 1.2.

2D
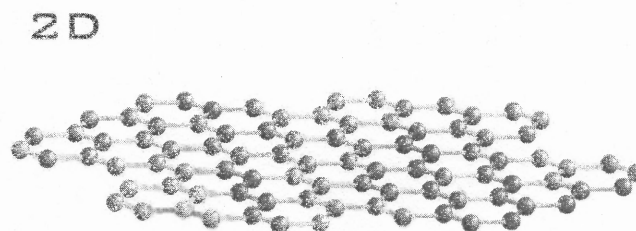
Figure 1.2 Two-dimensional structure of graphene [6].

c) One-dimensional Allotropes.

Carbon Nanotubes (CNTs) represent the one-dimensional allotrope of carbon. They are comprised of hollow cylinders of carbon atoms consisting of rolled tubes of graphite layers as shown in Figure 1.3. with the ends capped by half a fullerene cluster. There are two types of CNTs: single-walled carbon nanotubes (SWNTs) and multi-walled carbon nanotubes (MWNTs). As their names imply, SWNTs consist of a single, cylindrical graphene layer, whereas MWNTs comprise of multiply nested graphene layers telescoped around one another.

1D
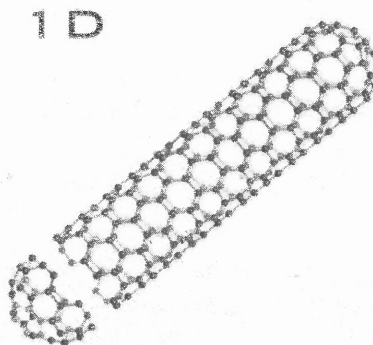
Figure 1.3 One-dimensional structure of a single wall carbon nanotube [6].

(d) *Zero-dimensional Allotropes*.

Fullerenes: The soccer ball shaped C_{60} fullerene is the best known example of an ideal zero-dimensional structure. It consists of 20 hexagonal and 12 pentagonal rings to give a cluster of icosohedral symmetry with a closed cage structure (Figure 1.4). Each carbon atom is bonded to three others and is sp^2 hybridized. C_{60} has two bond lengths – the 6:6 ring bonds can be considered "double bonds" and are shorter than the 6:5 bonds. C_{60} is not "superaromatic" as it tends to avoid double bonds in the pentagonal rings, resulting in poor electron delocalisation. As a result, it behaves more like an electron deficient alkene, and reacts readily with electron-rich species. The geodesic and electronic bonding factors in the structure account for the stability of the molecule. In theory, an infinite number of fullerenes can exist, their structure based on pentagonal and hexagonal rings, constructed according to rules for making icosahedra.
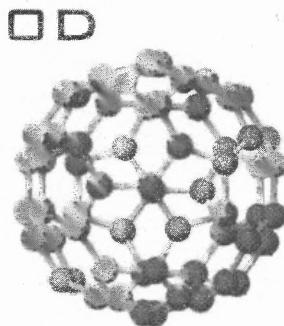

Figure 1.4. Structure of the C_{60} fullerene cluster [6].

1.3. Carbon Nanowalls

Carbon nanowalls (CNWs) are two-dimensional carbon nanostructures consisting of walls that are constructed of aligned graphene layers on different substrates. The CNWs

which are aligned almost vertically on the substrates (Figure 1.5) exhibit a lateral dimension of 0.1 to several microns and a thickness of several nanometers [13]. CNWs have been grown by plasma-enhanced chemical vapor deposition (PE-CVD) methods using gas mixtures of methane and hydrogen [6]. In the work reported in this thesis CNWs were grown by a radio-frequency PE-CVD technique using a more readily handled carbon precursor like ethanol mixed in with hydrogen, with and without a catalyst on the growth substrate.
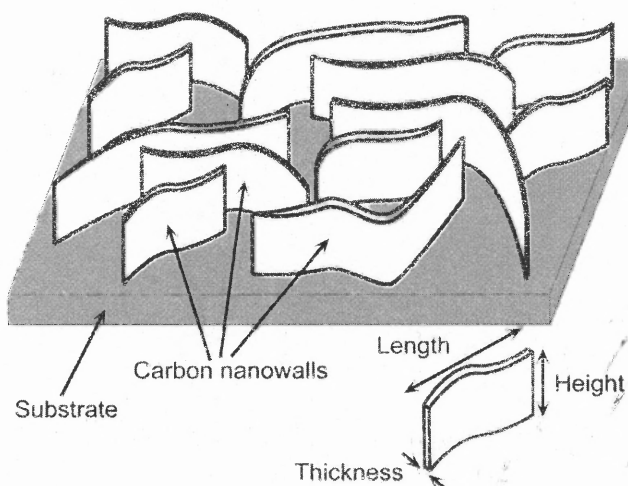
Figure 1.5 Structure of carbon nanowalls showing length, thickness and height [7].

1.4. Applications of Carbon Nanowalls

Nanowalls may have potential application in batteries, gas sensors, as catalyst support and super-hydrophobic coatings, and in light emission/detection, field emission and biomedical devices. They can also be used for electrochemical or adsorption-induced hydrogen storage [8]. Also studies are going on using substrates having carbon nanowalls as electrodes in an electrochemical cell such as a battery. This application is possible due

to the larger surface area of CNWs because a large surface area would provide high current density on the electrode surface.

CHAPTER 2

CHEMICAL VAPOR DEPOSITION

2.1 Fundamentals of Chemical Vapor Deposition (CVD)

Chemical vapor deposition involves the deposition of a non-volatile solid material on a suitably placed substrate from a gaseous phase. In a CVD process precursor gases (often diluted in carrier gases like argon as in the case of the experiments reported in this thesis) are delivered into the reaction chamber at near ambient temperatures. As they pass over or come into contact with a heated substrate, they react or decompose forming a solid phase which is then deposited on the substrate. The substrate temperature is critical and can influence what reactions will take place. A generic CVD reactor is shown in Figure 2.1.
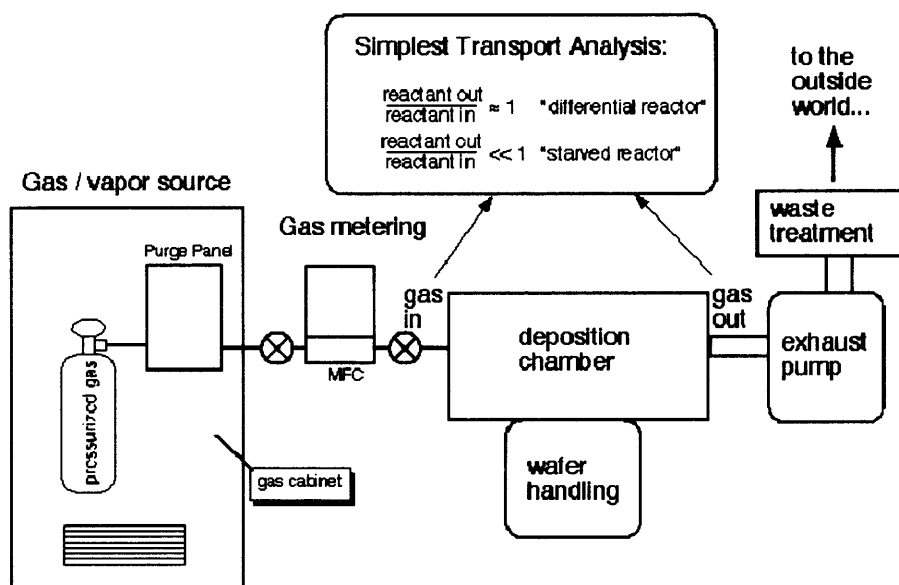
Figure 2.1 Schematic depiction of a generic CVD reactor.

2.2 Steps in a CVD Process

Once a reaction is identified, the following CVD process steps would typically occur:

a) Delivery of appropriate source gas

b) Transport of gas to substrate

c) Deposition of film:

      i) Adsorption of gas on substrate

      ii) Reaction on substrate

d) Transport of byproducts away from the substrate

Types of sources

a) Gases

b) Volatile liquids

c) Sublimable solids

d) Combination of above

Source materials should have the following properties:

a) Stable at room temperature

b) Sufficiently volatile

c) Reaction temperature should be lower than the melting point of the substrate

d) Capable of producing desired element or compound on substrate with easily removed by-products.

Growth of films depends on the following parameters:

a) Transport of a source gas to the deposition surface

b) Adsorption of gas on the substrate

c) Reaction on the substrate

d) Transport of by-product gases away from the substrate

2.3 Types of CVD

A number of CVD methods have been used. They differ in the techniques employed to initiate the chemical reactions leading to deposition and system parameters. Here are some of the general classifications:

a) Classified by operating pressure:

i) Atmospheric pressure CVD (AP-CVD) - CVD processes at atmospheric pressure.

ii) Low-pressure CVD (LP-CVD) - CVD processes at sub-atmospheric pressures.

iii) Ultrahigh vacuum CVD (UHV-CVD) - CVD processes at a very low pressure, typically below 10^{-6} Pa ($\sim 10^{-8}$ torr). Reduced pressures tend to reduce unwanted gas-phase reactions and improve film uniformity across the wafer. Most modern CVD process are either LPCVD or UHVCVD.

b) Classified by physical characteristics of vapor:

i) Aerosol assisted CVD (AA-CVD) - A CVD process in which the precursors are transported to the substrate by means of a liquid/gas aerosol, which can be generated ultrasonically. This technique is suitable for use with non-volatile precursors.

ii) Direct liquid injection CVD (DLI-CVD) - A CVD process in which the precursors are in liquid form (liquid or solid dissolved in a convenient solvent). Liquid solutions are

injected in a vaporization chamber by injectors (typically car engine injectors). Then the precursors vapors are transported to the substrate as in classical CVD process. This technique is suitable for liquid or solid precursors. High growth rates can be reached using this technique.

c) Plasma-assisted CVD

   i) Plasma-Enhanced CVD (PE-CVD) - CVD processes that utilize a plasma to enhance chemical reaction rates of the precursors. PE-CVD processing allows deposition at lower temperatures, which is often critical in the manufacture of semiconductors. Plasma can be generated by a dc power, radio frequency (RF) or microwaves known as microwave plasma-assisted CVD (MPCVD)

   ii) Remote plasma-enhanced CVD (RPE-CVD) - Similar to PE-CVD except that the wafer substrate is not directly in the plasma discharge region. Removing the wafer from the plasma region allows processing temperatures down to room temperature.

2.3 RF-Plasma Enhanced Chemical Vapor Deposition

The plasma is generally created by an RF frequency between two electrodes, the space between which is filled with the reacting gases. This technique was used in the work for this thesis to grow carbon nanowalls.

Why is a plasma used for deposition?

   A plasma is a gas in which a significant percentage of the atoms or molecules are ionized. Fractional ionization in plasmas used for deposition and materials processing varies from about 10^{-4} in typical capacitive discharges to as high as 5-10% in high

density inductive plasmas. Processing plasmas are typically operated at pressures of a few milliTorr to a few Torr, although arc discharges and inductive plasmas can be ignited at atmospheric pressure. Plasmas with low fractional ionization are of great interest for materials processing because electrons are light compared to atoms and molecules resulting in inefficient energy exchange between electrons and the neutral gas. Therefore the electrons can be maintained at very high equivalent temperatures – tens of thousands of degrees K, while the neutral atoms remain at ambient temperature. These energetic electrons can induce many processes that would otherwise be very improbable at low temperatures, such as dissociation of precursor molecules and the creation of large concentrations of free radicals.

The second benefit of deposition within plasma arises from the fact that electrons are more mobile than ions. As a consequence, the plasma is normally more positive than any object it is in contact with, as otherwise a large flux of electrons would flow from the plasma to the object. The voltage between the plasma and the objects it contacts is across a thin sheath region. Ionized atoms or molecules that diffuse to the edge of the sheath region feel an electrostatic force and are accelerated towards the object's surface. Thus, all surfaces exposed to the plasma receive energetic ion bombardment. The potential across the sheath surrounding an electrically isolated object (the floating potential) is typically only 10–20 V, but much higher sheath potentials are achievable by adjustments in the reactor geometry and configuration or by negatively biasing the object using a separate power supply. Thus, films can be exposed to energetic ion bombardment during deposition. This bombardment can lead to increased film density, removal of contaminants, and improvement of the film's electrical and mechanical properties.

Substrate Heater   Thermocouple
Gas Reservoir   Substrate
        Injector Head   Pump Head
Gas Manifold   RF Electrode   Plasma
        RF Power   Pumping
                            System
                            (Deposition/UHV)
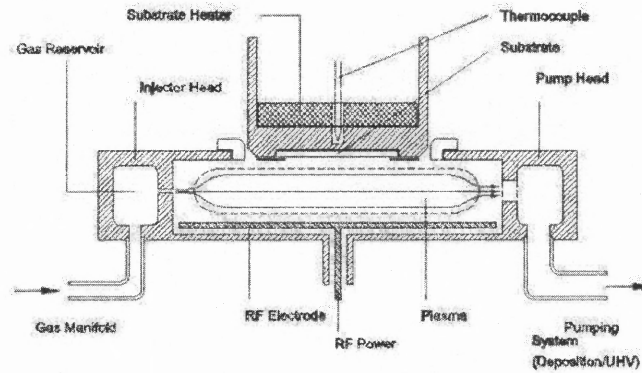
Figure 2.2 Schematic diagram of an RF-PE-CVD system.

RF-Plasma enhanced chemical vapor deposition (PE-CVD) is typically performed in a reactor at temperatures up to $1000^{\circ}C$ to form a film which is a product of a chemical reaction between the source gases supplied to the reactor. A plasma is generated in the reactor to increase the energy for the chemical reaction at a given temperature and the process is typically performed on one side of the substrate at a time. A schematic diagram of a RF-PE-CVD system is shown in Figure 2.2.

CHAPTER 3

EXPERIMENTAL DETAILS OF CNW GROWTH

Deposition of CNWs carried out on silicon, on silicon with Ni catalyst and on nickel foil (99.99% pure) using radio frequency-plasma enhanced chemical vapor deposition (RF-PE-CVD). Ethanol vapor carried by Ar gas bubbled through the liquid was used as the carbon source. Hydrogen gas was supplied to the reactor during the catalyst precursor reduction and growth of CNWs. The growth of CNWs was confirmed by field emission-scanning electron microscopy (FE-SEM), and by Raman spectroscopy using 632.8 and 785 nm laser excitation.

3.1 Preparation of Substrates

Silicon substrates (1 cm square) were cleaved form Si (100) wafers, washed by distilled water and then sonicated for 30 minutes in 10ml ethanol and 10 ml acetone solution. After sonication, the wafer was rinsed with distilled water and dried in air.

For Si substrates with Ni catalyst, nickel formate dihydrate (from Aldrich) was used as the catalyst precursor [9]. Its 5mM light green solution was prepared in 20 ml ethanol. A Si substrate, cleaned as described above, dipped into the catalyst precursor solution for 20 minutes, then taken out and placed in air for drying. It was observed that the deposition of the precursor on silicon was not uniform and there appeared to be small islands of the precursor on the wafer surface.

Ni substrates (1 cm square) were cut from nickel foil (99.99% pure), rinsed in, sonicated in ethanol and used for CNW growth.

3.2 CNW Growth Procedure
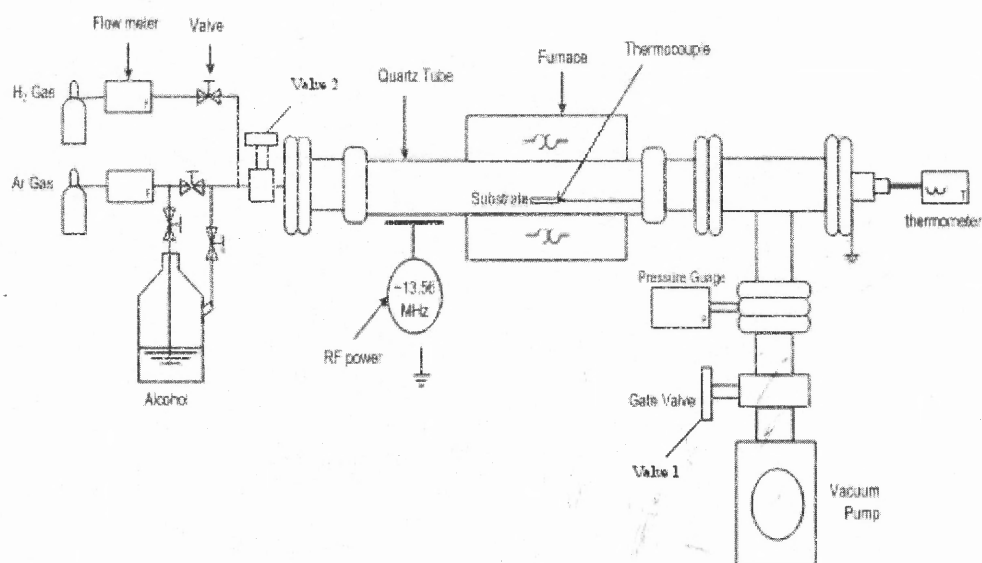
Figure 3.1 RF-PE-CVD system used for the growth of CNWs using ethanol as the carbon source [10].

An RF-PE-CVD system used for CNW deposition is shown schematically in Figure 3.1. The reactor tube length was 780mm and its diameter 254mm. The tube was evacuated by rotary pump with the gate valve (V1) at the reactor outlet controlling the pumping speed. A needle valve (V2) and the reactor inlet controlled the flow of gasses to the reactor. The pressure in the reactor tube was controlled by manually adjusting V1

and V2 valves. The gasses were supplied through a 3-way manifold combining three gas lines carrying argon, argon bubbled through liquid ethanol, and pure hydrogen. Each line was equipped with a flow meter and a control valve, so that the flows could be adjusted independently.

The substrates were placed in center of the reactor tube, the vacuum pump was turned on, valve V1 was closed and the gate valve V2 was opened fully so that all the air in the system could be pumped away. After pumping for approximately 30 min the following two process steps were carried out, depending on the substrate type: 1. Reduction of the catalyst precursor (only for Si substrates with catalyst), 2. Deposition.

1. Reduction

The temperature was set initially at 250° to 300°C [9] and allowed to rise at a rate of 10°C per minute. The valves in the gas manifold were adjusted for hydrogen flow in at a rate of 20 sccm (standard cubic centimeters per minute) and argon at a flow rate of 4 sccm. The pressure was maintained at 0.8 Torr. Temperature of 500 °C was maintained for 30 minutes.

2. Deposiiton

Once the catalyst precursor has been reduced, the temperature was raised further at approximately 10°C/min rate. The hydrogen flow rate was increased to 30 sccm [11]. The ethanol bubbler valve was opened to allow a flow rate of 15sccm and the pure argon valve was completely closed The RF generator was turned on and its output power adjusted for 200 W with reflected power of approximately 70 W. Discharge in the gas was observed as a pale reddish color. The needle valve V2 was opened completely and

the gate valve was adjusted so that the pressure inside the tube was 300-400 mTorr. The deposition temperature was controlled between 850 and 890°C and deposition was carried out for 1 hour.

After deposition hydrogen, Plasma and bubbled ethanol supply was turned off. Valve V1 was opened completely and the pure argon supply was opened to cool down the system quickly. Once the system was cooled to room temperature, the argon supply and the vacuum pump was turned off. The sample was then taken out of the reactor.

Samples on silicon substrates with precursor showed a shiny mirror-like surface. Similarly in case of Nickel, the surface was completely black over the whole region.

CHAPTER4

SCANNING ELECTRON MICROSCOPY AND RAMAN SPECTROSCOPY RESULTS AND DISCUSSION

Carbon nanowalls have been grown on three different substrates using the RF-PECVD technique discussed in Chapter 3. It has been found that the pressure conditions between 0.30 to 1.1 Torr are favorable for growth. It was also observed that that the pressure have minimal effect on CNW growth as long as the hydrogen and bubbled ethanol partial pressure ratio is 2:1, as determined by the flow rates are 30 and 15 sccm, respectively.

4.1 Scanning Electron Microscope Images and Analysis

CNWs has been observed by a LEO field-emission scanning electron microscope (FE-SEM) and Raman spectroscopy on three different substrates – a clean silicon wafer, a silicon wafer with catalyst and a pure nickel foil. The FE-SEM images showing growth of CNWs on a silicon wafer without catalyst, a silicon wafer with catalyst and a nickel foil substrate are shown in Figures. 4.1 – 4.3. The SEM images clearly show the formation of carbon nanowalls with vertical alignment, very similar to those reported by Yoshimura et al [7]. Raman spectra, discussed on section 4.3, confirms this assertion. The area of growth of CNWs also depended on position of the substrate in the quartz tube of the RF-PE-CVD reactor, except in case of the nickel substrate. The reason might be that nickel itself acts as the active catalyst for CNW growth. Furthermore, it appears that the

catalytic role in the formation of CNWs because it was possible to grow CNWs on silicon wafers without a catalyst (Figure 4.1). By comparing the SEM images in Figures. 4.1 – 4.3, not much difference is observed in the morphology and density of the CNWs grown on the two types of substrates.
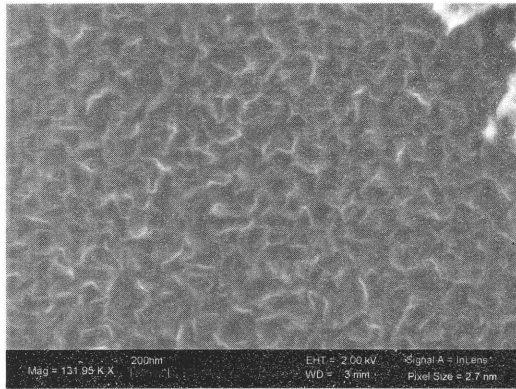
Figure 4.1 SEM image of CNWs on a pure silicon wafer.
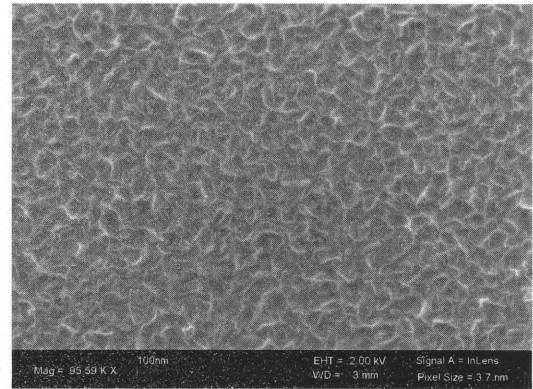
Figure 4.2 SEM image of CNWs on Silicon with catalyst.
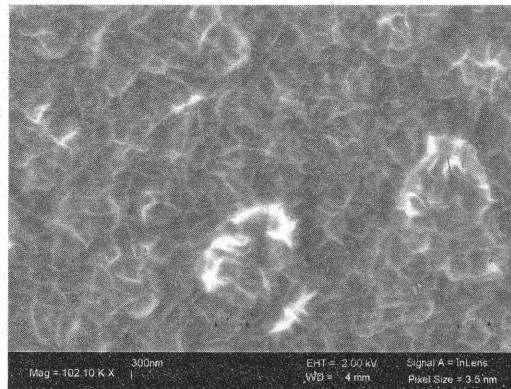
Figure 4.3 SEM image of CNWs on a pure nickel foil.

4.2 Raman Spectroscopy

Raman spectroscopy was carried out using a Mesophotonics SE 1000 Raman spectrometer with a 250 mW near-infrared laser emitting at 785 nm and a 130 µm diameter spot size. The system operates with automated XYZ stage and video camera for visualization of the sample. Typical acquisition time used was 10 sec. Raman spectra were also obtained using a confocal Jobin Yvon LabRam micro-Raman spectrometer with a 20 mW He-Ne laser source emitting at a wavelength of 632.8 nm focused to a spot size of 10 µm with a 10x lens. The Raman data obtained from samples prepared in this work were compared with the Raman spectra on CNWs from Yoshimura *et al* [7] and Ni *et al* [12], and on graphene layers obtained by Ferrari *et al* [13]. The Raman spectra of graphene differs from that of graphite crystals in two regions. Firstly, in the disordered (D) mode region around 1300 cm^{-1}, shown in Figure 4.4 using 514.5 nm laser excitation taken from the edge of a crystal of graphite and a graphene layer, a broad line resolvable into two components is seen in graphite, whereas in graphene, the line shifts down in frequency and only a single peak is observed. Secondly, in the second order 2D mode region around 2600 cm^{-1} region, a broadened doublet is seen for graphite and a single line is observed for 1-layer graphene as shown in Figure 4.5.
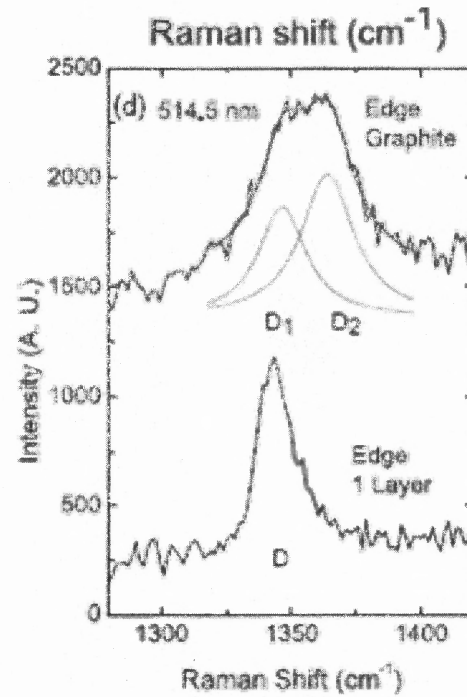
Figure 4.4 Raman spectra in the D mode region from graphite and 1-layer graphene [13].
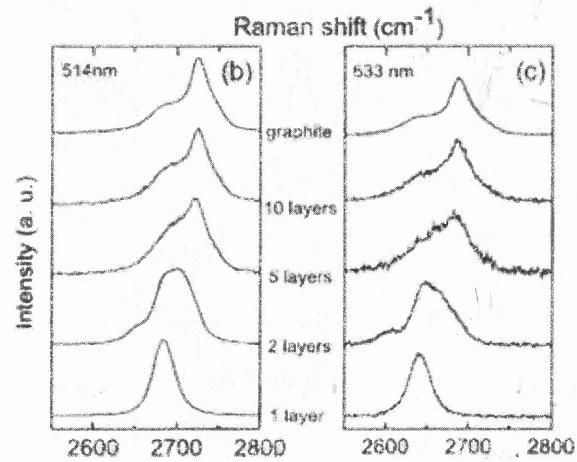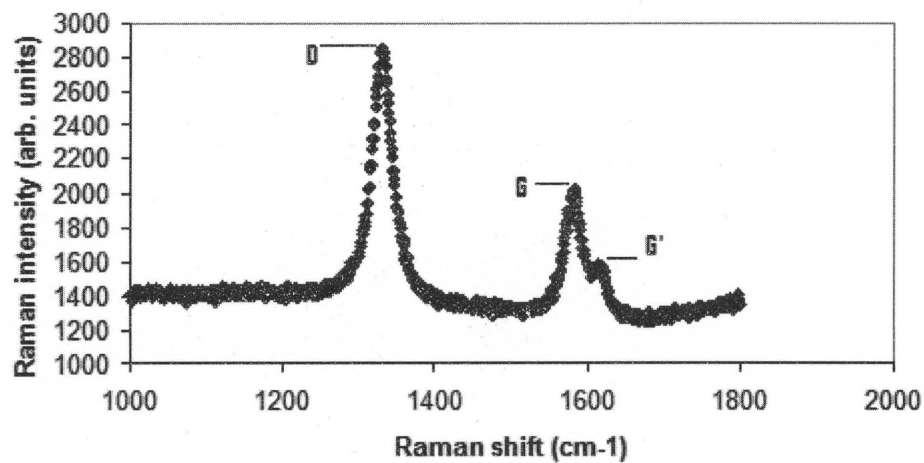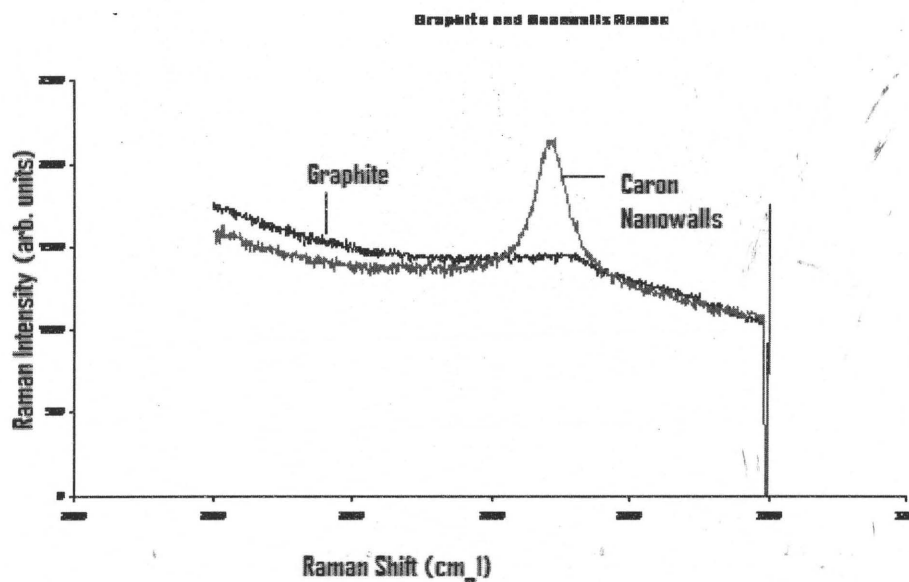

Figure 4.5 Raman spectra in the 2D mode region from graphite and 1- and 2-layer graphene excited with 514 nm and 633 nm laser radiation [13].
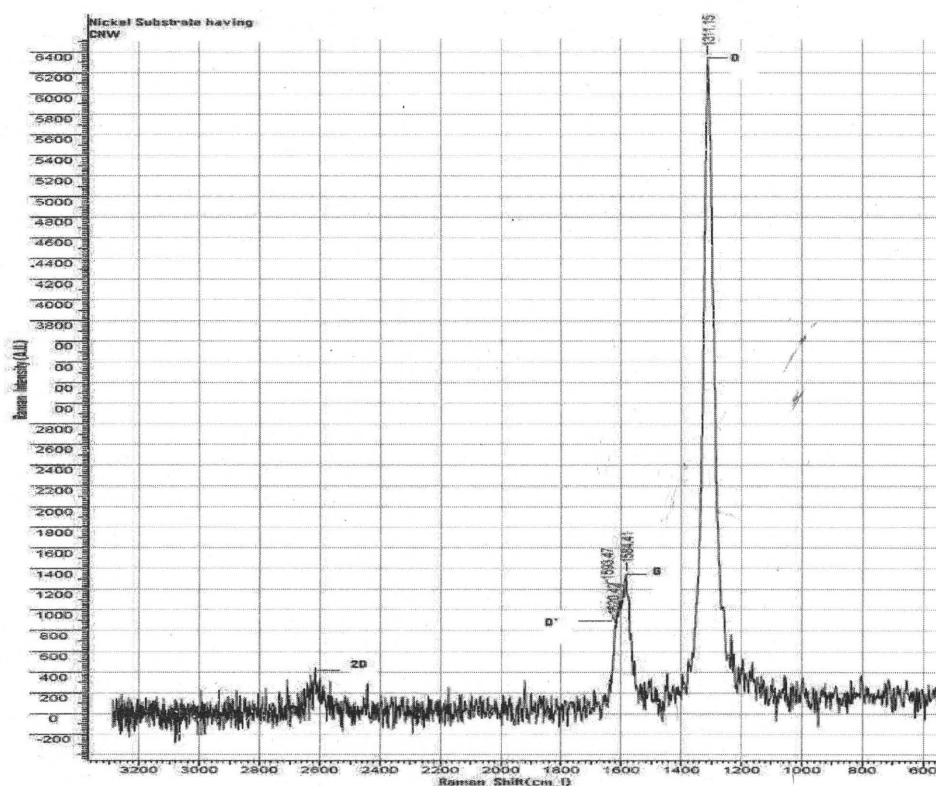
Figure 4.6 Raman spectrum of CNWs on nickel prepared in this work in the D, G and D' mode region using 632.8 nm excitation.

Figure 4.7 Raman spectrum of CNWs prepared in this work and HOPG graphite using 632.8 nm excitation in the 2D region.

Figures. 4.6 and 4.7 show the 632.8 nm Raman spectra of CNW samples on nickel prepared in this work in the D (1320 cm^{-1}), graphitic G (1580 cm^{-1}) and second order D' (1620 cm^{-1}) mode, and 2D mode (2600 cm^{-1}) regions, respectively. The 2D spectrum of HOPG graphite excited with 632.8 nm radiation is also shown in Figure 4.7. Figure4.8 shows 785 nm laser excited Raman spectrum in the 600 to 3200 cm^{-1} range for CNWs on nickel.

Figure 4.8 Raman spectrum of CNWs on nickel prepared in this work in the 600 to 3200 cm^{-1} region using 785 nm excitation.

The observation of an intense D line which increases in intensity with increasing wavelength of the exciting laser radiation, is in agreement with prior Raman results on

CNWs published by Yoshimura et al [7] and Ni et al [12]. This is consistent with the FE-SEM images (section 4.2), which show the formation of CNWs which shows the morphologies very similar to that observed by these authors. The high intensity and relatively narrow linewidth of the D line is likely to be a consequence of the vertical alignment of the CNWs on the substrate. This orientation allows the electric vector of the incident laser beam in the backscattering arrangement to couple strongly with defects lying perpendicular to the plane of the carbon walls. The observation of a single 2D line downshifted with respect to the 2D line envelope observed in HOPG graphite (Figure 4.7) when compared with the 2D mode data for single layer graphene from Ferrari et al [13] in Figure 4.5 suggests that the CNWs are constructed of "bricks" comprised of one or two layers of graphene. Further support of this interpretation comes from the observation of a relatively narrow single D line similar to that seen in single layer graphene by Ferrari et al [13] (also see Figure 4.4). The lateral dimension or length of the walls as defined by Yoshimura et al [7] can be estimated from their plot of the ratio of the intensity of the D line and the G line (I_d/I_g) obtained using 532 nm laser excited Raman data. The average value of the CNW length of a typical sample prepared on nickel is estimated to be 0.4 μm after correcting for the laser excitation used. This value is consistent with approximate values obtained from the SEM images.
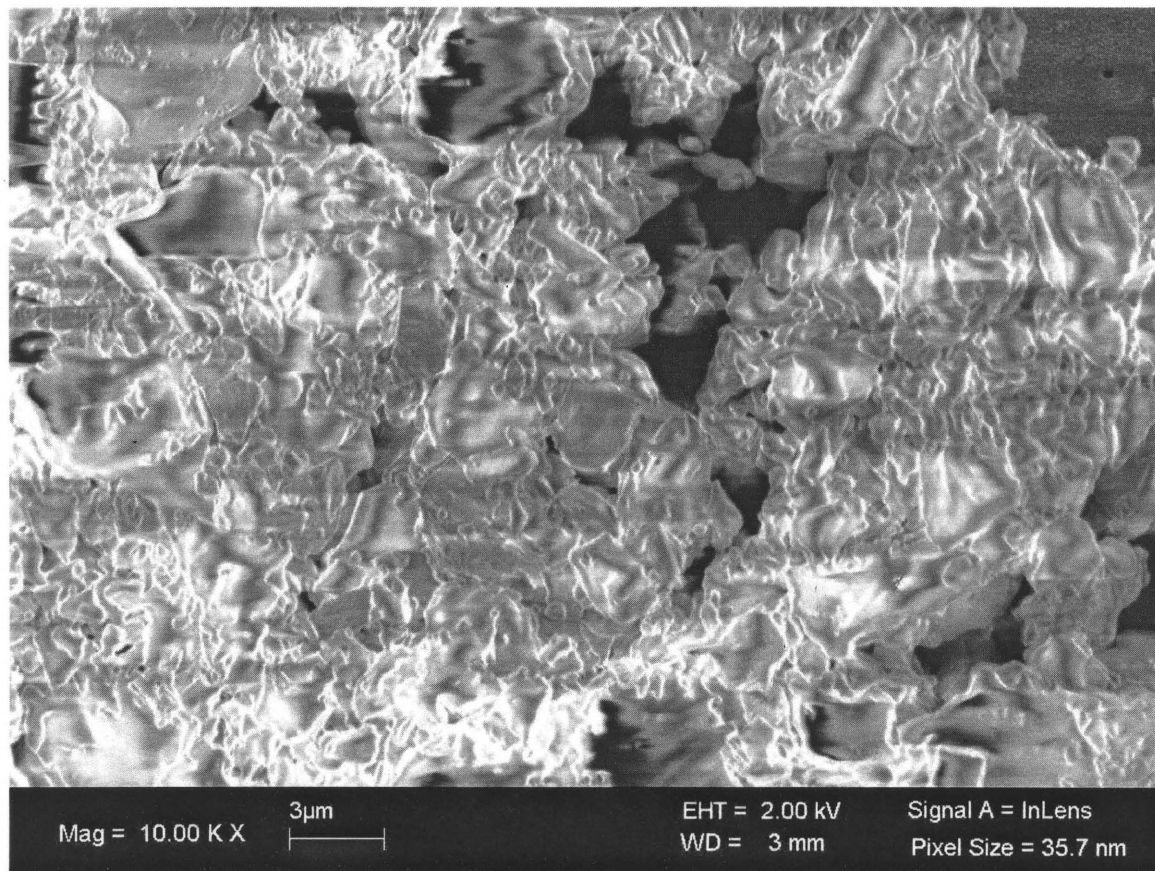
4.3. Conclusion

It has been shown for the first time that CNW growth occurs when ethanol is used instead of methane as the carbon source. The Raman results also indicate that the carbon walls

are composed of one or two layers of graphene and have an average length of 0.4 μm. High temperature on the reactor walls and substrate, and the application of an RF plasma converts ethanol in the presence of hydrogen to carbon and OH radicals, and H^+ ions [14]. It is worth noting that the only parameter that differentiates the growth of CNWs from the growth of carbon nanotubes is the high concentration of H^+ ions in the plasma.
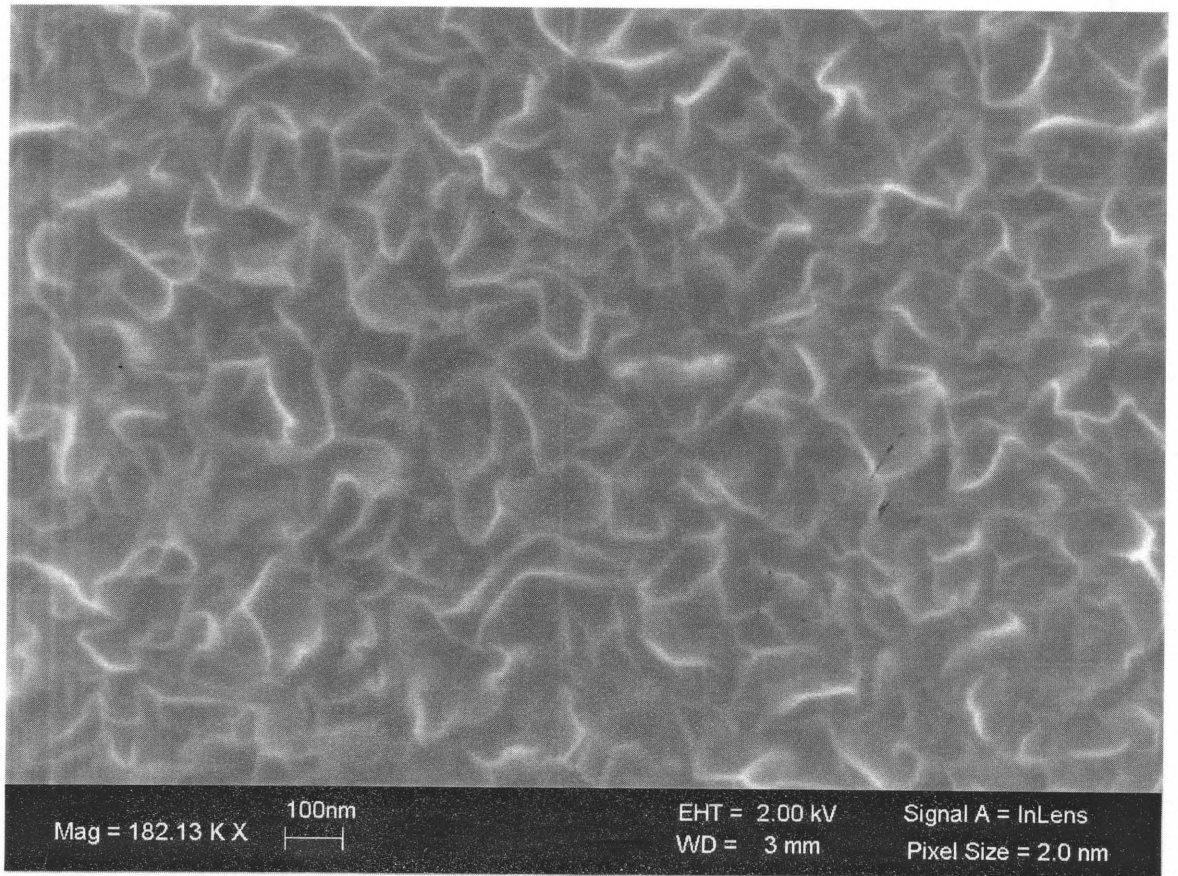
APPENDIX A

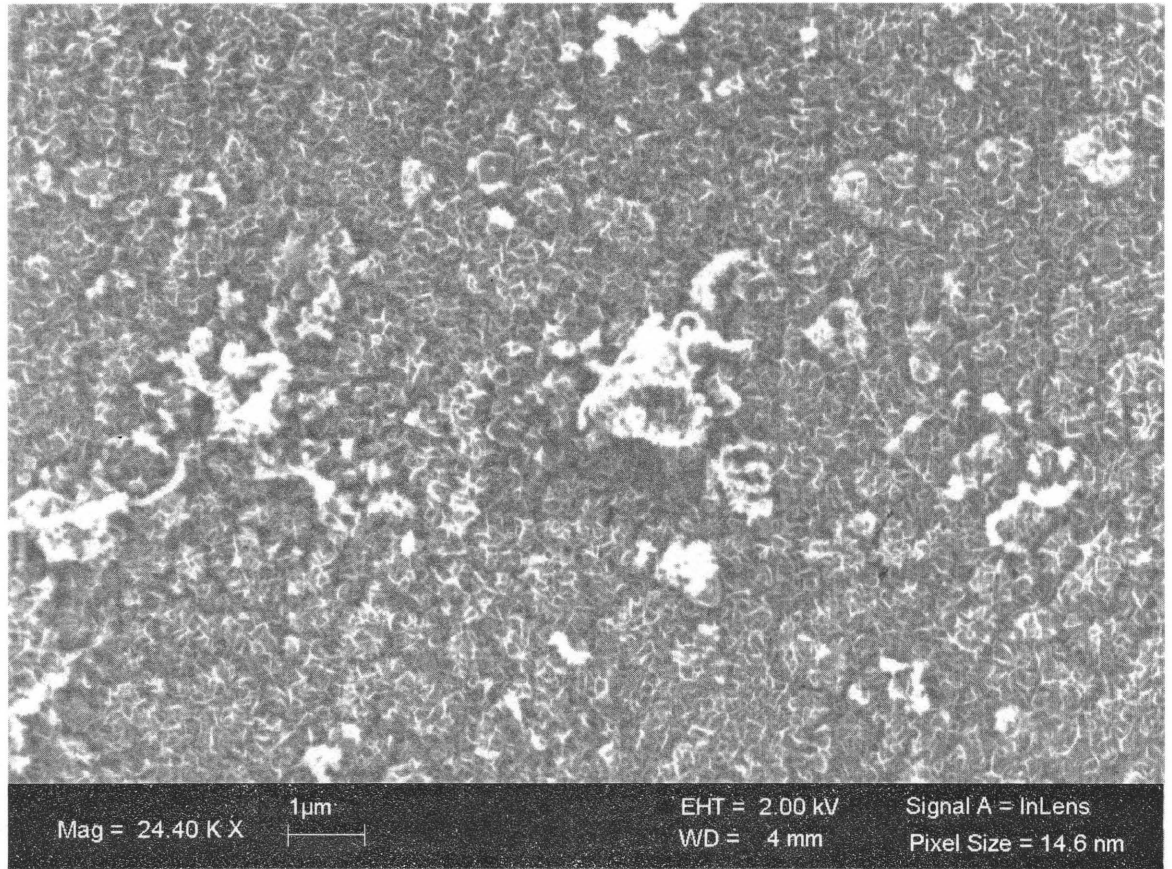## SEM PICTURES

SEM images of CNWs grown on different substrates.

Mag = 10.00 K X   3µm   EHT = 2.00 kV   Signal A = InLens
                                      WD = 3 mm   Pixel Size = 35.7 nm

Figure A.1 SEM image of CNW on Silicon Substrate having catalyst taken from 3micro meter.

Mag = 20.00 K X   1µm   EHT = 2.00 kV   Signal A = InLens
                          WD = 3 mm   Pixel Size = 17.8 nm
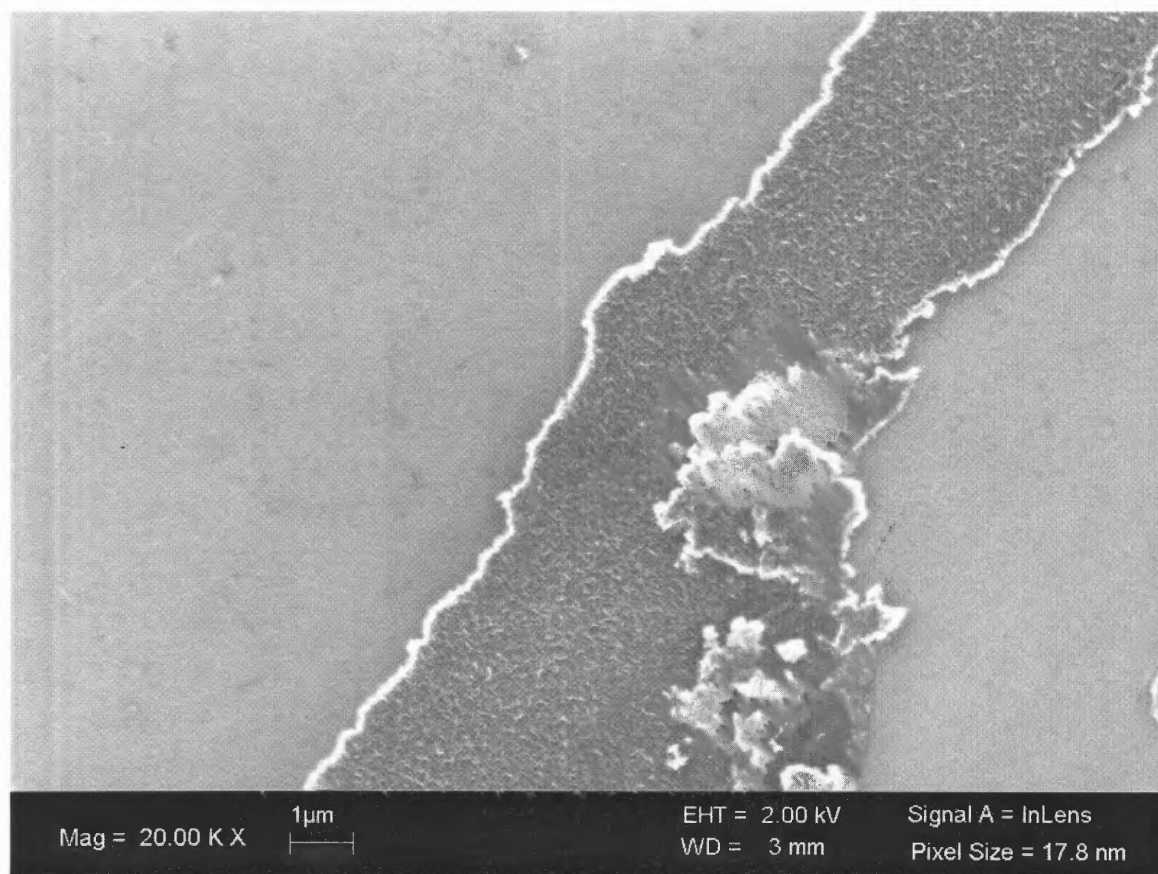
Figure A.2 SEM image of CNW ON Silicon Substrate having catalyst, showing specific growth of CNW.

Mag = 182.13 K X   100nm   EHT = 2.00 kV   Signal A = InLens
                             WD = 3 mm   Pixel Size = 2.0 nm

Figure A.3 SEM image of CNW on Silicon Substrate having catalyst, taken from 100 nm.

Mag = 24.40 K X   1μm   EHT = 2.00 kV   Signal A = InLens
WD = 4 mm   Pixel Size = 14.6 nm

Figure A.4 SEM image of CNW on Nickel Foil, taken at 1 micro meter.
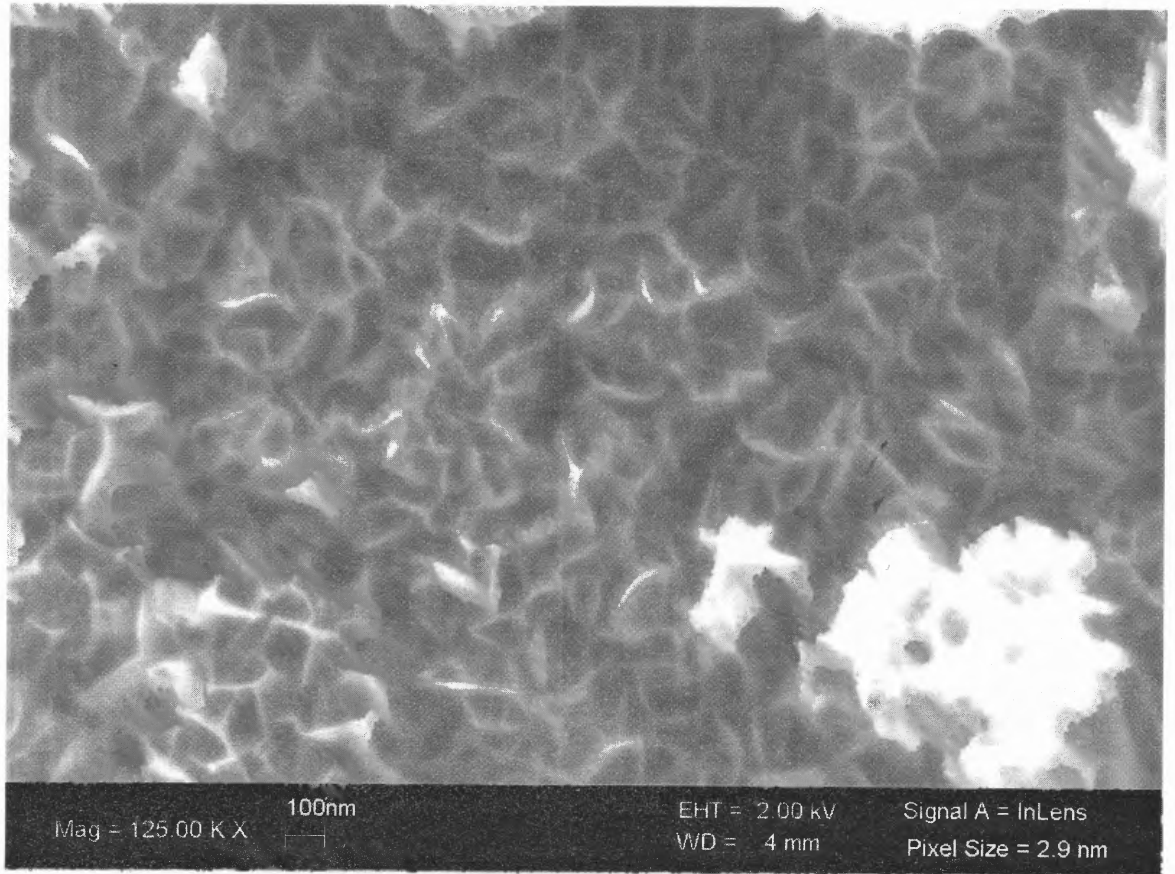
Figure A.5 SEM image of CNW grown on Nickel Foil, taken from 100nm.
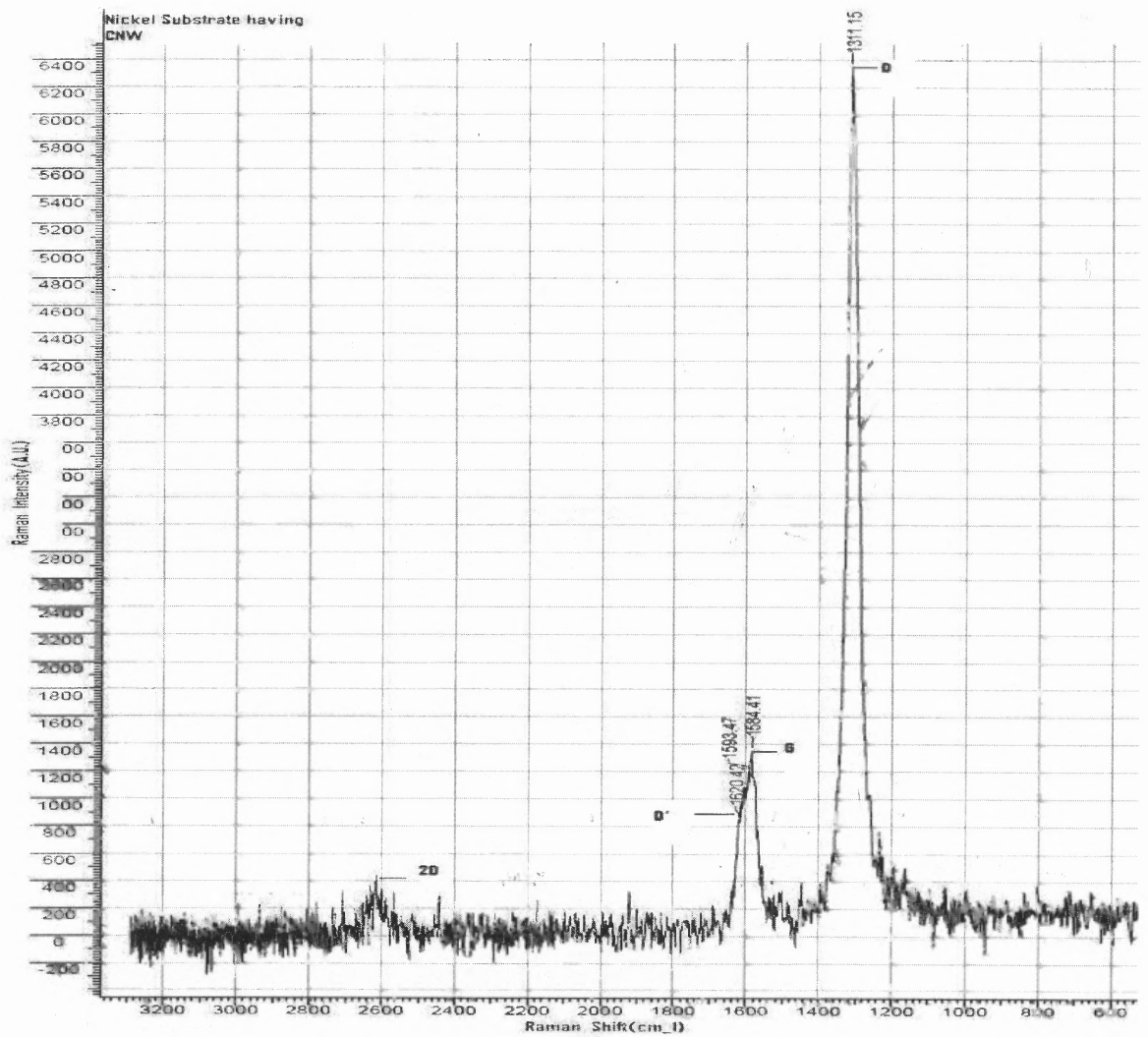
Raman Spectra of Substrates having CNWs.

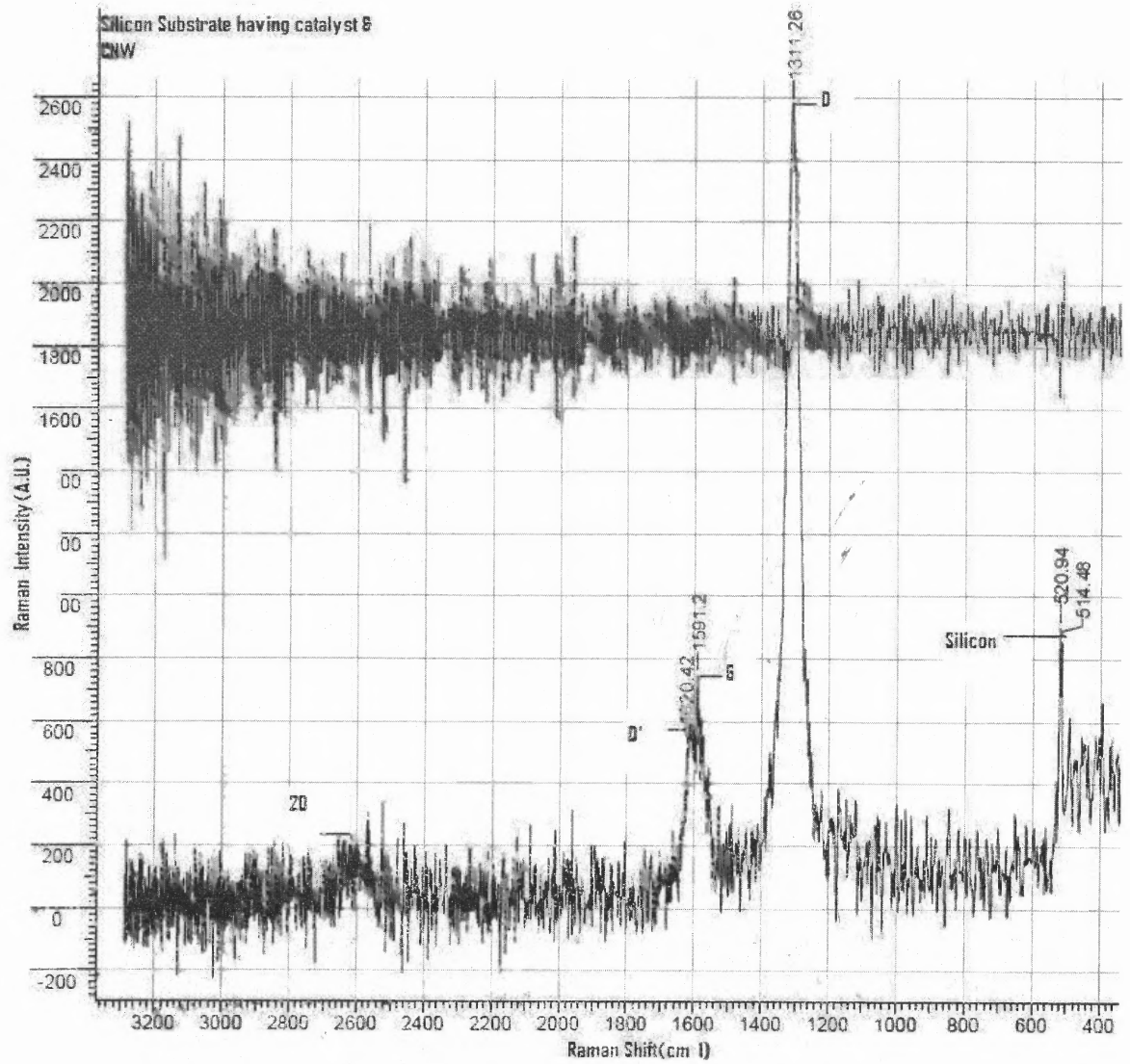**Figure B.1** Raman Spectrum of CNW grown on Nickel foil.

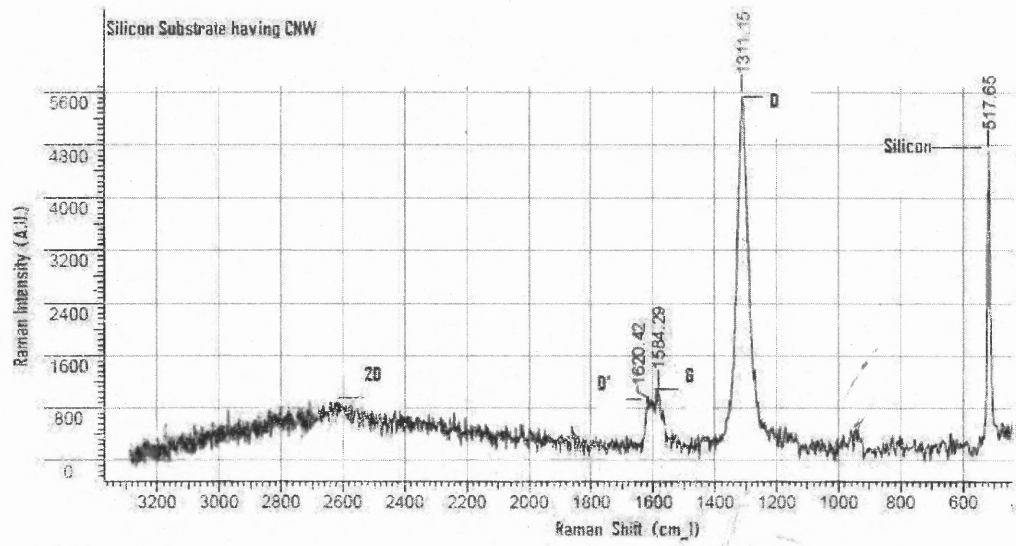**Figure B.2** Raman Spectrum of CNW grown on Silicon Wafer having Catalyst.

Figure B.3 Raman Spectrum CNW grown on Silicon Wafer.

REFERENCES

[1] M. S. and Dresselhaus, "G. Intercalation compounds of graphite," *Advanced Physics,* volume 51, pp. 1–186, 2002.

[2] K. S. *et al,* Novoselov, "Electric field effect in atomically thin carbon films," *Science,* volume 306, pp. 666–669, 2004.

[3] C. *et al,* Berger, "Electronic confinement and coherence in patterned epitaxial grapheme," *Science,* volume 312, pp. 1191–1196, 2006.

[4] D. Muller, Li, M. B., Gilje, S., Kaner, R. B. and Wallace G. G, "Processable aqueous dispersions of graphene nanosheets," *Nature Nanotech,* volume 3, pp. 101–105, 2008.

[5] Geim, A. K. & Novoselov, K. S. "The rise of graphene," *Nature Mater,* volume 6, pp. 183–191, 2007.

[6] M. I. Katsnelson, "Graphene: Carbon in Two Dimensions," *Materials Today,* volume 10, pp. 1-2, 2007.

[7] A. Yoshimura, S. Kurita, M. Tachibana, K. Kojima, P. Molina-Morales and H. Nakai, "Fabrication of Carbon Nanowalls by DC Plasma Enhanced Chemical Vapor Deposition and Characterization of Their Structures," *Proceedings. 5th IEEE Conference. on Nanotechnology,* Nagoya, 2005

[8] K. Jurewicz, E. Frackowiak, F. Beguin, "Towards the Mechanism of Electrochemical Hydrogen Storage in Nanostructured Carbon Materials," *Applied Physics,* volume 78, pp. 981-987, 2004.

[9] J. Geng, H. Li, V. B. Golovko, D. S. Shephard, D. A. Jefferson, and B. F. G. Johnson, "Nickel Formate Route to the Growth of Carbon Nanotubes," *J. Phys. Chem.B,* volume 108, pp. 18446-18450, 2004.

[10] C. Yu, S. C.Wang, M. Sosnowski and Z. Iqbal, "Plasma Enhanced Chemical Vapor Deposition of Polyperinephtalene Thin Films," *Synthetic Metals,* pp. 1, 2008.

[11] M. Hori, M. Hiramatsu, K. Shiji and H. Amano, "Fabrication of Vertically Aligned Carbon Nanowalls using Capacitively Coupled Plasma Enhanced Chemical Vapor Deposition Assisted by Hydrogen Radical Injection," *Applied Physics Letters,* volume 84, number 23, pp. 1-3, 2004.

[12] Z. H. Ni, H. M. Fan, Y. P. Feng, Z. X. Shen, B. J. Yang, and Y. H. Wu "Raman spectroscopic investigation of carbon nanowalls," *Journal of Chemical Physics,* volume 124, pp. 204703, 2006

[13] A. C. Ferrari, J. C. Meyer, V. Scardaci, C. Casiraghi, M. Lazzeri, F.. Mauri, S. Piscanec, D. Jiang, K. S. Novoselov, S. Roth and A. K. Geim, "Raman Spectrum of Graphite and Graphene layers," *Physics Review Letters,* volume 97, pp. 187401, 2006.

[14] M. Hiramatsu, M. Hori, "Fabrication of Carbon Nanowalls," *Journal of Physics*, pp. 248-249, 2005.